SLAC–PUB–9073

November 2001

Photon Background in DIRC Fused Silica Bars *

A. Yarritu, S. Spanier, J. Va'vra
Stanford Linear Accelerator Center, Stanford, CA 94309, USA.

presented at

2001 IEEE
Nuclear Science Symposium
and
Medical Imaging Conference
San Diego, California
4 – 10 November, 2001

Abstract

The DIRC (acronym for **D**etection of **I**nternally **R**eflected **C**herenkov radiation) is the ring imaging Cherenkov detector of the BaBar detector at the Pep-II ring of SLAC. The Cherenkov radiators consist of 4.9 m long rectangular fused silica bars each glued together from four equal pieces. The photon detector is a water tank equipped with an array of 10,752 conventional photomultipliers. The current study attempts to identify sources of photonic background generated in the DIRC bars. A conclusion of this work is that there are two major sources: one such component consists of photons created by the delta-ray electrons in the fused silica, which in turn can produce Cherenkov light. The second component comes from the reflections of photons from the EPOTEK-301-2 glue-fused silica interface while they are traveling in the bars. The reflection occurs because of a slight mismatch of the refraction indices.

*Work supported by Department of Energy contract DE–AC03–76SF00515

1 Introduction

For the study of CP violation at BaBar it is important to flavor tag B mesons via the identification of charged kaons from their decay in the momentum range up to 3 GeV/c. To analyze B decays it is necessary to separate charged pions (protons) from charged kaons for momenta up to 4.2 GeV/c. The DIRC performs well for these tasks and achieves a separation in Cherenkov-angle mean values of better than 3σ until 3 GeV/c and about 2.5σ at the highest momenta. Even though the performance of the signal is well understood by the BaBar Monte Carlo [1] only 60% of the observed photonic background sources are identified. Therefore, the photonic background produced in the fused silica bars needs to be studied in more detail. The machine background fom Pep-II is highly suppressed by the precise timing of the arrival of the signal photons. First indications for a background component generated in the bars come from an analysis of BaBar DIRC data [2]. Here we use a dedicated experimental setup to separate the Cherenkov from the photonic background-light production by cosmic rays [3]. The conclusion of our study is that there are two major mechanisms which contribute to such background. These are Cherenkov photons generated by delta rays originating from the primary charged particle (cosmic muon) and reflections from the EPOTEK-301-2 glue/fused silica interfaces.

We argue that scintillation light is negligible for the following resons:

- A direct measurement of the scintillation in fused silica with a Fe^{55} source yields a negligible amount of photons.
- The measured rate of photon background generated by cosmic-ray muons in a 4 m long bar is mostly explained with the aforementioned two mechanisms as shown by our detailed Monte-Carlo program.
- The arival time distribution of the scintillation light does not reproduce the measured time spectrum assuming an isotropic source.
- The solid angle acceptance in the quartz bar for the randomly emitted scintillation photons is very small.

2 Experimental Setup

The experimental setups are shown in Fig. 1. Three standard DIRC bars with dimensions 17 mm×31 mm×1225 mm are glued together with EPOTEK-301-2 glue [4] where the glue joint has a thickness of 25 μm. A photomultiplier (PMT) type Quantacon XP2020 Philips [5] is attached directly to each of the bars with the EPOTEK-301-2 glue. On this side light passes through the subsequent surfaces fused silica, EPOTEK-301-2 glue, Borosilicate glass, and the bi-alkali photocathode. In setup 1 (a), the bar end opposite to the photomultiplier is equipped with a mirror which is air coupled with a spring applying pressure against the bar.

The charged particle tracks enter the bar with an angle of 56 degrees with respect to the bar normal and some 50 cm distance to the left bar end in Fig. 1, pointing away from the

phototube. The particle trajectory is defined by two entrance scintillation counters aligned with an uncertainty in the angle of about 1^0 which are in coincidence with one exit counter below the bars. The 12¨ thick lead shielding in front of the exit counter provides a selection of the minimum muon energy to be ~ 0.4 GeV.

The track angle ensures that all internally reflected Cherenkov light first travels through the bar away from the PMT and reflects on the mirror before it arrives in the phototube. This leaves a time window of about 36 ns for collecting light from the bar in front of the Cherenkov signal. In setup Fig. 1 (b), the Cherenkov photons are efficiently absorbed by the photon trap, so that a study of the background photons which would normally arrive in coincidence with the Cherenkov peak is possible, essentially extending the observation time interval to 70 ns. The photon trap is an aluminium box coupled to the bar with a pipe surrounding the bar end. Both devices are filled with a fluid which matches the refraction index of fused silica and their walls are covered with photon-absorbing cloth.

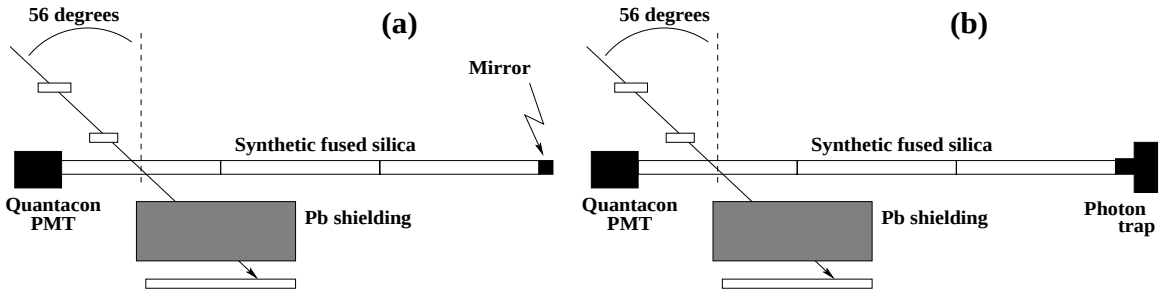

Figure 1: Experimental setups used to study the photon background. The Cherenkov signal propagates to either (a) the mirror or (b) the photon trap. In the former case, a window of ~ 36 ns is available to study the early photon background activity before the Cherenkov signal returns; in the latter case a ~ 70 ns window is available.

2.1 Data

The PMT signal was amplified $\times 10$ with a LeCroy fast amplifier and the output recorded with a HP digital scope read out by a MAC IIcx computer with CAMAC-based GPIB interface. The Fig. 2(a) and Fig. 2(b) show the raw waveforms for a single event with the mirror and the photon trap, respectively. In Fig. 2(a) one clearly observes the Cherenkov signal arriving at channel number 375. The earlier activity in front of that channel can be attributed to background photons. In Fig. 2(b) the Cherenkov signal is absorbed efficiently by the photon trap. The remaining pulses slowly diminish towards the end of the 70ns window.

A pulse-finding algorithm was applied offline: the waveform is differentiated channel by channel and a peak is localized if the waveform starts dropping for at least 5 consecutive channels. The result was checked with a deconvolution algorithm which takes the single-photon pulse shape into account. In addition the application of a LeCroy TDC allowed to make a leading edge "single hit" determination which was reproduced by applying this

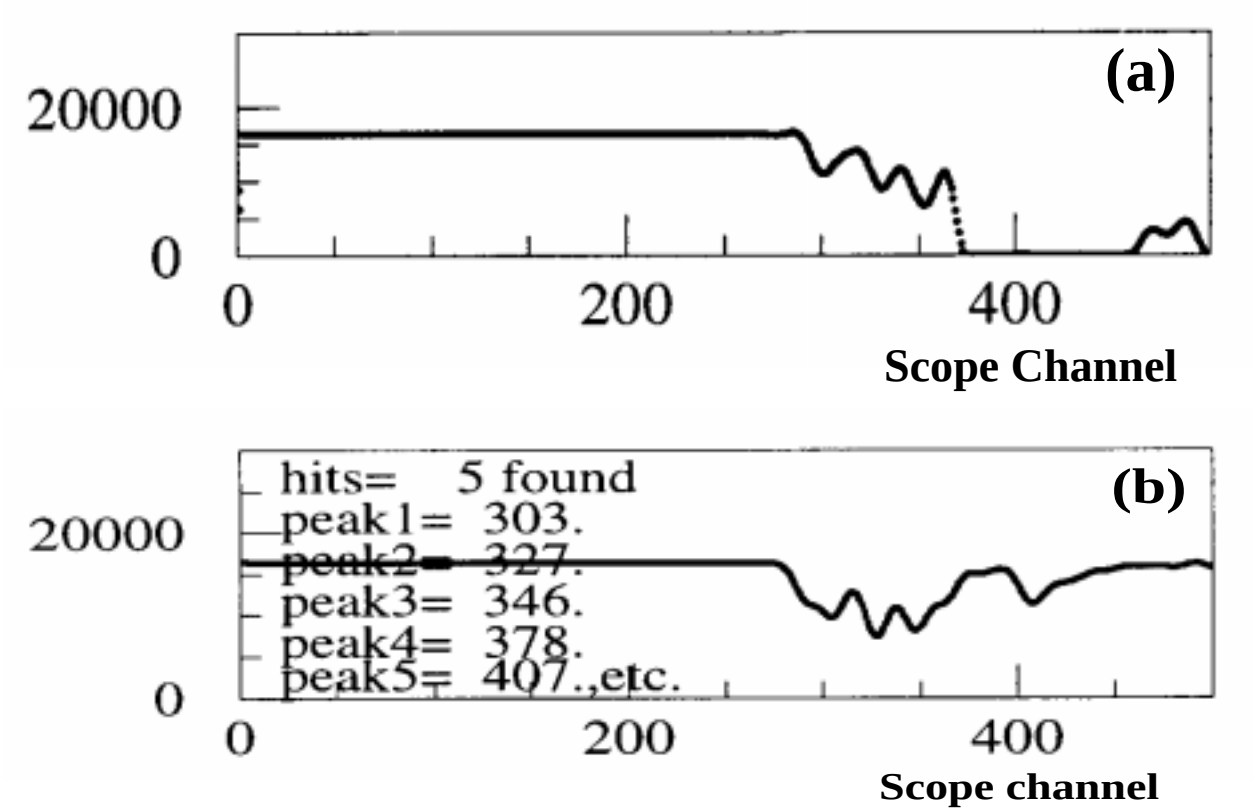

Figure 2: Digital scope output from a single event for the mirror setup (a) and the photon-trap setup (b). The horizontal axis is time in terms of scope channels (1 scope channel = 0.4 ns) and the vertical axis is the amplitude. In (a) one notices the large Cherenkov pulse arriving at channel 375 and the background pulses arriving earlier. In (b) there is a distinct lack of the large Cherenkov pulse. The background pulses fade away as one approaches 70ns. (The text is the output of the peak finding algorithm displaying the location of each photon hit)

algorithm to the recorded pulse shapes. We did not find further significant improvement in the sensitivity of our analysis using the other methods. Figure 3 shows the result of the pulse-finding algorithm for the mirror setup. The Cherenkov pulse clearly arrives about 36 ns after a very first activity peak near channel 115 which is due to delta-ray electrons traveling fast enough to produce Cherenkov photons by themselves in somewhat randomized directions. As will be discussed later, the shoulder at channel 130 is explained by the reflection of photons at the first glue plane.

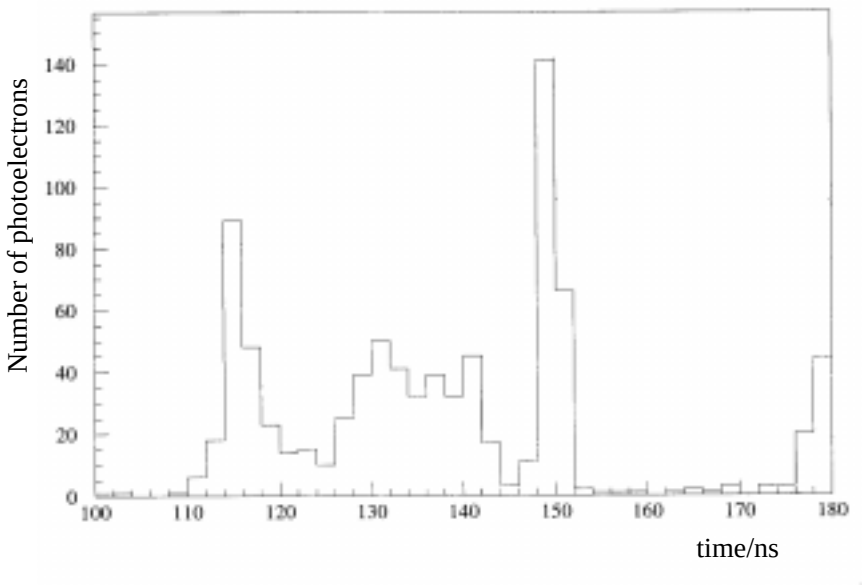

Figure 3: Measured time distribution of photon pulses obtained from the peak finding algorithm using the mirror data. The Cherenkov signal arrives at channel 150. The hits before this time are all considered background.

3 Supplemental Measurements

3.1 Measurement of Reflectivity of EPOTEK-301-2 glue

The index of refraction of the EPOTEK-301-2 glue as a function of wavelength was measured in a separate experiment using four different laser wavelengths. Based on the results for the TE mode the Fresnel reflectivity at a particular wavelength is calculated. The reflectivity was also directly measured with a 442 nm laser [6]. The reflectivity as a function of the angle of incidence to the surface quartz-glue for the different methods is shown in Fig. 4. The curve calculated from the refraction-index measurement is systematically too low. For our Monte Carlo simulation we adjusted the TE mode to describe the distinct features of the arrival-time spectrum in the data. This yielded the curve in in Fig. 4 which is consistent with the measured values of the reflectivity.

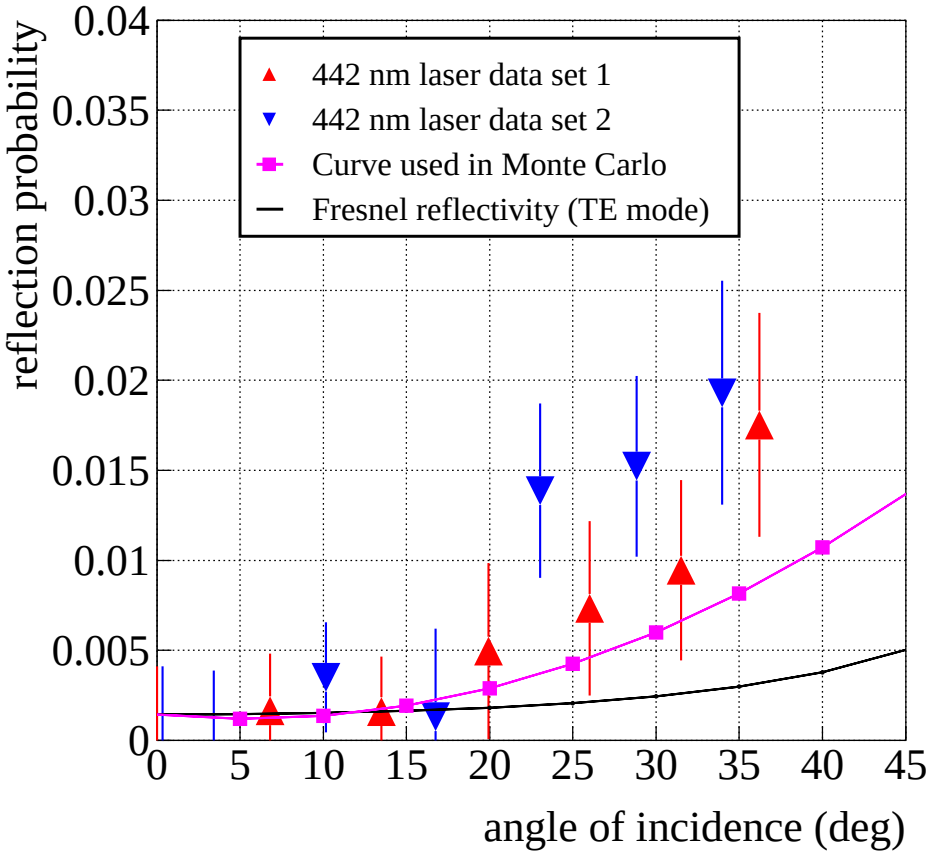

Figure 4: The Fresnel curve is based on the measurement of the index of refraction. Also shown is the data from two different measurements of the reflectivity per bounce from the glue/silica interface. Finally, the curve with square references is used in the Monte-Carlo program that simulates the 4m long bar cosmic ray experiment mentioned in section 2.

3.2 Measurement of Scintillation

The scintillation rate of quartz was measured with a Fe^{55} source which primarily emits 5.9 keV X-rays. Its emission of energetic gamma rays, which can create Compton electrons with enough energy to produce their own Cherenkov photons, is negligible. In addition, the 5.9 keV photons will only produce scintillation light by the photoelectric effect: the X-rays have enough energy to kick off a bound electron, which can then travel to nearby atoms and excite them, thus producing scintillation photons. From a source directly placed on the bar a rate of $(1.96 \pm 0.3) \cdot 10^3$ counts/min was observed in the PMT next to it. According to the Monte Carlo simulation the PMT acceptance was 5%. Therefore, the probability for a single 5.9kEV X-ray to produce a scintillation photon is $2.7 \cdot 10^{-4}$. Since the activity of the Fe^{55} source was $1.46 \cdot 10^8$ counts/min, the scintillation rate per MeV is $4.5 \cdot 10^{-2}$ counts/MeV. Assuming that all of the energy deposited by the traversing muon is used to create scintillation photons (the minimum ionizing muon deposits 13.5 MeV) there would be 0.03 detected scintillation photons per muon. This number is negligible compared to the ≈ 5 observed background photons in a time window of 0-70 ns.

4 Monte Carlo

We simulated both experimental setups described in section 1 based on the Monte-Carlo program of a single DIRC bar geometry [7] which generates a photon-wavelength spectrum according to the quantum efficiency of the photomultiplier and traces photons from their point of generation through the bar taking into account wavelength dependent bulk-material attenuation, bar surface scattering and mirror reflection (photon absorption). Cherenkov light is generated for all charged particles above their Cherenkov threshold. We implemented delta-ray generation from the primary particle track using the FLUKA package [8] and the optical properties of the glue.

4.1 Delta-Ray Simulation

The light yield originating from delta rays only is shown in Fig. 5 together with the data from our mirror setup. We do not account for the signal finding efficiency in the Monte Carlo (100%). Therefore, we reduce the Monte Carlo spectrum to match the heighest entry in the data. It is evident that delta rays describe the time behaviour of the earliest background photons in the 30 ns window in front of the signal while the overall spectrum is not well reproduced. It is interesting to note that scintillation photons emitted in random direction along to the particle track arrive at a similar time spectrum only that their rate is strongly suppressed compared to delta rays.

4.2 Reflectivity of Glue

It is obvious from Fig. 5 that delta rays do not explain the background features satisfactorily. The distance to the first glue-joint between the bars corresponds roughly to the 15 ns where

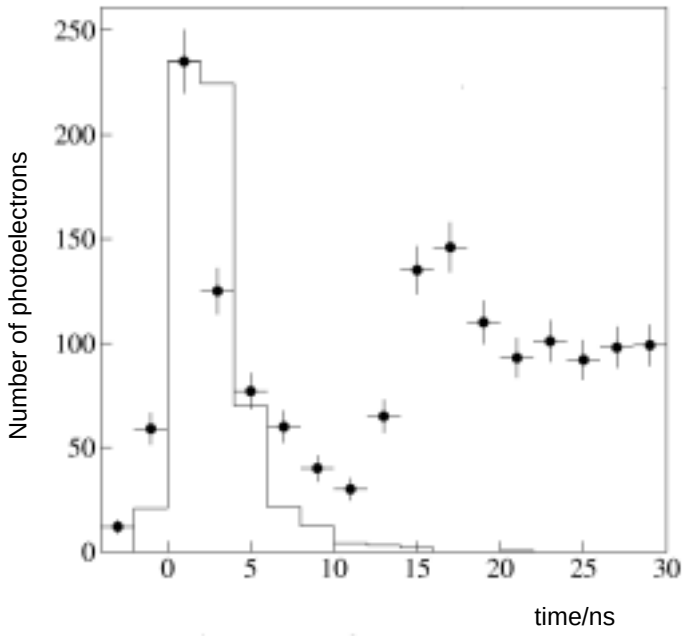

Figure 5: Light yield from simulated delta rays: Monte Carlo is represented by the smooth line, the data by the dots. Delta rays are the dominant component in the first background photon peak.

the shoulder shows up in the data. We included the reflection of photons from the glue/fused silica interfaces which so far was neglected in the DIRC simulations. The modified spectrum is shown in Fig. 6 together with both the mirror and photon-trap data, since they agree in their characteristics within the first 30 ns. The Monte Carlo was again normalized to the first peak in the spectrum requiring a factor 0.6 and the ratio between the second "reflection" peak and the first "delta-ray" peak was tuned using the reflectivity per angle of incidence (see Fig. 4).

The analysis of the reflection was done as follows. (a) First, we have used our value of the refraction index of glue [6] and that of fused silica, and calculated the TE and TM reflections using the Fresnel theory. In this case, the second peak in Fig. 6 was underestimated by a factor of five. (b) Second, we have tried to tune the refraction index of the glue to obtain the best agreement with the 4m-long bar data. Again, we calculate TE and TM modes appropriately according to Fresnel theory. However, following this procedure, we have obtained unphysical values of the refraction index of the EPOTEK-301-2 glue. (c) Third, we have used the fit to the direct measurement of the reflectivity of the glue/fused silica interface in TE mode at 442 nm. In this case, the Monte Carlo exaggerated the size of the second peak in Fig. 6. (d) Finally, we decided to tune the fit to the direct measurement of the reflectivity to achieve agreement with the data in Fig. 6. The result of this tuning is shown in Fig. 4. The tuned curve is still consistent with the measured data. In summary we believe that the reflection at the glue/fused silica interface may not follow the simple Fresnel theory. In fact the deviation from this theory may point to a more complex situation at the

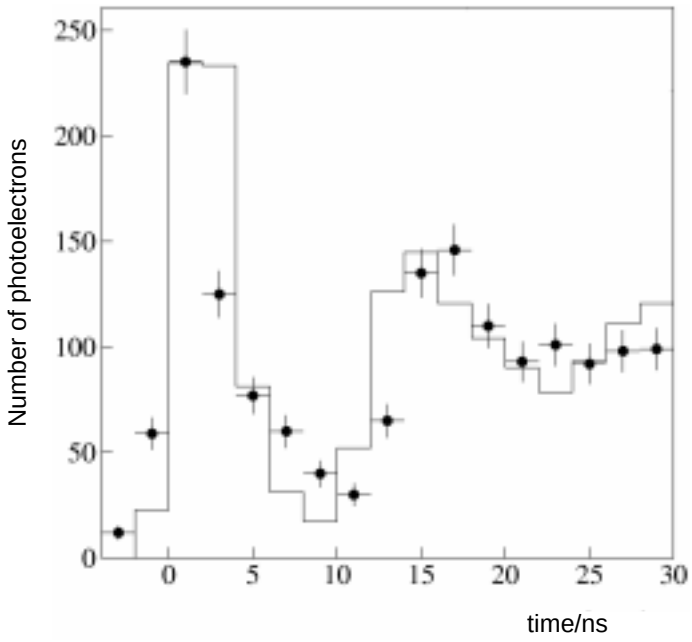

Figure 6: Time distribution of photon background pulses in the first 30 ns. The data (a combination of both the mirror and photon trap data) is represented by the dots and the Monte Carlo by the smooth line. The Monte Carlo was normalized to the data using a factor of 0.6.

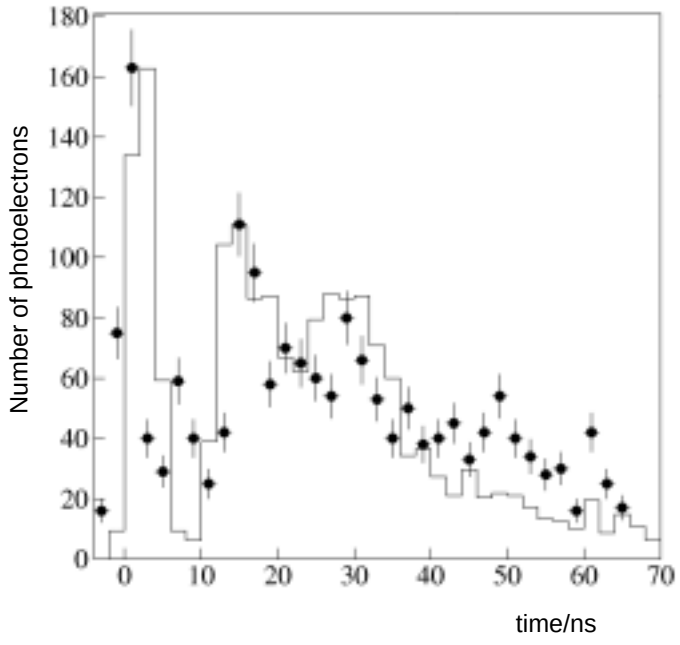

Figure 7: Time distribution for the photon-trap data (dots) and Monte-Carlo simulation (line) of the full 70 ns time interval. The normalization factor is slightly higher compared to the 30 ns set (Fig. 6) due to the inefficiency of the photon trap.

interface between bars. This is under investigation.

Fig. 7 shows the photon-trap data extending the time interval without a Cherenkov-light signal to 70 ns together with the Monte Carlo generated with our tuned reflectivity curve. The basic features of the distribution are reproduced well. It shows, that nearly all background photons are collected within the 70 ns.

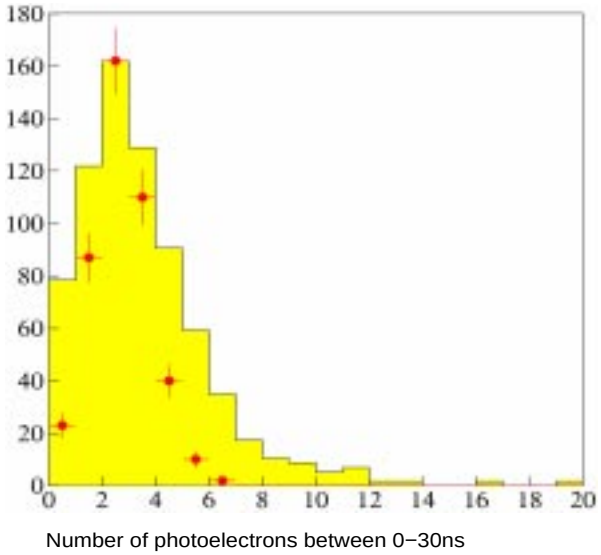

Figure 8: Multiplicity distribution of background photons for the mirror setup (30 ns), Data (dots) and Monte Carlo (histogram) agree well in terms of the most probable number 3.

Using our adjusted Monte Carlo we determine that the most probable number of background photons in the first 30 ns is 3. For the full 70 ns interval the number of background photons is 5. We expect about 96 photoelectrons from the Cherenkov signal at the dip angle of 56^0, so that the most probable number represents $\approx 5\%$ to the proper DIRC Cherenkov signal. However, the distribution has a long tail caused by the delta-ray contribution as shown in Fig. 8. Since the real data have a finite pulse shaping time there is a natural upper limit on the number of pulses one can measure and the tail is suppressed.

5 Conclusion

We have shown that two major contributions to the photon background in DIRC fused silica bars in the BABAR experiment are (a) Cherenkov photons generated by delta-ray electrons and (b) reflection of all photons from the silica/glue interfaces. The reflection is caused by the difference in the refraction index of the glue and fused silica. The light yield due to scintillation is negligible.

Acknowledgments

We would like to thank B. Ratcliff for interest and suggestions. A technical help to build the experimental setup of R. Reif and M. McCulloch was very much appreciated. Contributions in the initial phase of J. Shawitz are also valued. The work was supported by Department of Energy contract DE–AC03–76SF00515 (SLAC).

References

[1] I. Adam et al. (DIRC Collaboration),
Operation of the Cherenkov Detector DIRC at High Luminosity,
presented at IEEE 2000 Conference, Lyon, France; SLAC-Pub 8783

[2] M. Benkebil and F. Wormser,
"Study of the DIRC Background During the First BaBar Cosmic Ray Run",
Internal DIRC Note# 125, July 1999.

[3] K. Yarritu, S. Spanier and J. Va'vra,
"Photon Background in DIRC Fused Silica Bars",
Internal DIRC Note # 141, September 19, 2001.

[4] EPOTEK-301-2 glue

[5] Quantacon XP2020, Philips

[6] J. Va'vra,
"Measurement of EPOTEK-301-2 Optical Glue Refraction Index and a Reflectivity from EPOTEK-301-2/Fused Silica Interface",
Internal DIRC Note # 140, July 2001.

[7] B. Ratcliff and S. Spanier,
"DIRC Dreams",
talk given at the 3rd International Workshop on Ring Imaging Cerenkov Detector (RICH 98), Ein Gedi, Dead Sea, Israel 1998, Nucl. Inst. Methods A 433, 456 (1999), SLAC-PUB-8064 (1999).

[8] A. Fasso, A. Ferrari, J. Ranft, and P. Sala
FLUKA99 program CERN, http:fluka.web.cern.chfluka